CHEMICAL ENGINEERING TRANSACTIONS
VOL. 62, 2017
A publication of AIDIC
The Italian Association of Chemical Engineering
Online at www.aidic.it/cet
Guest Editors: Fei Song, Haibo Wang, Fang He

ISBN 978-88-95608- 60-0; **ISSN** 2283-9216
DOI: 10.3303/CET1762192

High Open-circuit Voltage Perovskite Solar Cell Based on $CH_3NH_3PbBr_3$ Light Absorber Using Hole-conductor-layer-free Structure

Jinkui Song, Feihong Huang, Jianyou Chen, Shuangshuang Liu, Kun Cao, Mingkui Wang*

Wuhan National Laboratory for Optoelectronics, Huazhong University of Science and Technology, Wuhan 430074, China
mingkui.wang@mail.hust.edu.cn

In the present work, high open-circuit voltage perovskite solar cells based on the TiO_2/Al_2O_3/carbon structure have been prepared using simple screen printing method combined with drop-casting a $CH_3NH_3PbBr_3$ solution. The obtained device acquired 7.1 % efficiency with 1.33 V open-circuit voltage under AM 1.5G illumination by control the perovskite solution concentration, annealing temperature, annealing time and TiO_2 mesoporous layer thickness. The obtained perovskite device had almost no hysteresis under different scan rate, showing excellent steady state power output and stability.

1. Introduction

Solar cells could settle the growth demand for clean energy and solve a serious issue of environmental matter. Some solutions have been reported for avoiding the use of unstable organic HTMs. On one hand, the stable inorganic HTMs such as Li et al. has reported MoOx and VOx , which replace the organic HTMs (Li et al., 2015). On the other hand, Stranks S.D. et al. has reported HTM-free PSCs, which was fabricated due to the unique ambipolar property of perovskite materials that can serve as both a light absorber and a hole conductor(Stranks et al.,2013). Hole carriers in perovskite could be effectively extracted by Ag or Au electrodes, which could remove the unstable organic HTM layer to improved PSCs' stability. Cao K. et al. has reported that prepared the porous carbon electrode covered on inorganic metal oxide TiO2/Al2O3 layer. Compared to the smooth interface of the perovskite/electrode, hole carriers could be more effectively extracted by carbon counter electrode (Cao et al, 2015). The structure of TiO2/Al2O3/Carbon in the low-cost materials, simple process, lower equipment requirement etc. are impressive compared with Au electrode. And Mei A. et al. has reported that porous carbon electrode help to enhance device stability (Mei et al., 2014).
Owing to the enormous advantage, this structure has attracted extensive attention. And PSCs with high open circuit voltage have received great concern due to their prospect in applications such as driving electrochemical reactions: Schreier M et al. has reported carbon dioxide reduction and Luo J.et al. has reported photolytic wate and tandem solar cell (Schreier et al., 2015; Luo et al, 2014).
In perovskite solar cells, the devices' Voc is mainly determined by perovskite materials' electron and hole quasi-Fermi level. And its' voltage loss is mainly derived from the charge recombination and the Ohmic contact energy level barrier difference where interface of the electron / hole transport material in contact with the perovskite materials. Therefore, there are many researches that mainly control the open circuit voltage from the perovskite material itself and the interface optimization.
Herein, the above issues of HTM and high open-circuit voltage will be addressed by using carbon electrode in the HTM-free PSCs based on $CH_3NH_3PbBr_3$ perovskite material. Firstly, we fabricated mesoporous membranes that the structure is FTO/compact TiO_2(c-TiO_2)/mesoporous TiO_2(m-TiO_2)/mesoporous Al_2O_3(m-Al_2O_3)/ carbon counter electrode(Carbon) by screen printing technique. Secondly, we made $CH_3NH_3PbBr_3$ perovskite absorber with simple one-step method using $CH_3NH_3PbBr_3$ as precursor and then instilled the precursor through carbon counter electrode penetration into TiO_2/Al_2O_3 mesoporous layers. After optimizing

Please cite this article as: Jinkui Song, Feihong Huang, Jianyou Chen, Shuangshuang Liu, Kun Cao, Mingkui Wang*, 2017, High open-circuit voltage perovskite solar cell based on ch3nh3pbbr3 light absorber using hole-conductor-layer-free structure, Chemical Engineering Transactions, 62, 1147-1152 DOI:10.3303/CET1762192

the $CH_3NH_3PbBr_3$ perovskite solution concentration, annealing temperature, annealing time and TiO_2 mesoporous layer thickness. An encouraging V_{oc} of 1.33 V with PCE of 7.11% was obtained.

2. Experiment

2.1 Material synthesis

The synthesis method of CH_3NH_3I and CH_3NH_3Br as follows: In a 250-mL round bottom flask, 30 mL of methylamine solution (40% methanol solution) was added and placed in an ice bath at 0°C followed by the slow addition of 32.3mL of HI solution (57 wt% aqueous solution) or 23.32mL of HBr solution (48wt% aqueous solution) followed by stirring for 2h. After completion of the reaction, the solution was taken out at 50°C with a vacuum rotary evaporator to obtain a white powder. The product was dissolved with ethanol and the ether was added dropwise and precipitated and repeated three times. And finally vacuum drying to obtain CH_3NH_3I and CH_3NH_3Br white crystals.

2.2 Mesoscopic PSCs device preparation

Preparation of mesoporous TiO_2 layer: TiO_2 paste (Dyesol 30NRD) diluted with terpineol (dilution ratio of weight ratio of 1: 3.5, stir well). The TiO_2 paste was printed on an FTO / compact-TiO_2 substrate using a 400-mesh screen printing screen and dried at 125°C for 10 minutes. After cooling to room temperature, the slurry prepared by Al_2O_3 (Aladdin 30 nm) was screen printed on a mesoporous TiO_2 film by the same process and dried at 125 °C for 10 minutes. The TiO_2/Al_2O_3 mesoporous film was then sintered by heating in a process using air. The heating process was maintained at 112°C for 5 minutes, at 175°C for 5 minutes, at 350°C for 10 minutes, at 400 ° C for 15 minutes and at 500°C for 30 minutes. After cooling to room temperature, the carbon paste was printed onto Al_2O_3 in the same manner and heated to 400°C for 30 minutes. Finally, twelve templates were obtained by screen printing on FTO glass at a size of 5cm×10cm. The area of each battery is 0.56cm^2. The thickness of the mesoporous TiO_2 film is 500 nm, the mesoporous Al_2O_3 has a thickness of 800 nm and the thickness of the porous carbon electrode is about 10 μm. The thickness of each mesoporous layer during the preparation was tested by a step meter (DEKTAK, VEECCO, Bruker).

$MAPbI_3$ perovskite material injection: prepared 1M $MAPbI_3$ perovskite solution, with 10 μL of the pipette to take 2~3 μL perovskite solution drops to the blank mode, so that the free diffusion of perovskite solution. 70 degrees heating for 30 minutes to complete the preparation of $MAPbI_3$ perovskite battery.

$MAPbBr_3$ perovskite material injection: prepared the $MAPbBr_3$ perovskite solution, with 10 μL of the pipette to take 2~3 μL perovskite solution drops to the blank mode. So that free perovskite solution diffusion. After annealing, the preparation of $MAPbBr_3$ perovskite battery was completed.

3. Results and discussion

We first studied the perovskite solution into the mesoporous pattern in the different annealing time. By means of XRD test, as shown in figure S1, the XRD patterns was the best annealed 30 minutes. So, we choose 30 minutes annealing time as we optimized condition. Under the annealed 30 minutes, in the case of all conditions were the same, we studied the different annealed temperature. Compared to the XRD patterns from figure S2, we choose 70 °C as we optimized condition. From figure S2 we can see until 70°C the peak intensity of XRD patterns was the best with the annealed temperature raise up, the peak intensity become stronger. Later, with the temperature raise up the peak intensity of XRD patterns begin to decline. When the annealed temperature reached 110 °C, impurity peak of XRD patterns began to appear. This suggests that the $MAPbBr_3$ perovskite began to decompose. When the annealed temperature reached 130 °C and annealed 30 minutes, the perovskite basic decomposition.

Then, we studied the concentration of the solution. The XRD of different concentration as shown in figure S3. We studied three concentrations respectively were 0.6 M, 0.8 M, and 1 M. From figure S3a we can find strong peak intensity using 0.8 M concentration solution. It indicated that the perovskite crystal face had good consistency. At the same time, we used normalization method with handling figure S3a data to get figure S3b. We can see 0.8 M concentration XRD patterns have minimum peak width at half height. That showed the concentration of 0.8 M perovskite solution crystallization quality was better.

We can summary through the above experiment. $MAPbBr_3$ crystallization conditions is ideal while the $MAPbBr_3$ solution concentration is 0.8 M, heating temperature is 70 °C and heating time is 30 minutes.

Figure 1a illustrates the device structure employing the TiO_2/Al_2O_3/carbon scaffold. That the mesoporous Al_2O_3 layer is applied between the porous TiO_2 and carbon counter electrode(CE) for preventing the direct contact between TiO_2 and carbon. The mesoporous Al_2O_3 film serve as spacer layer to separate the TiO_2 and carbon CE for preventing electron-hole recombination at the TiO_2 and carbon CE interface. The devices' energy levels for the three layers are illustrated in Figure 1b. Once the $MAPbBr_3$ fills the mesoporous layers. It

will generate free charge carriers in this material by light stimulates. And free charge carriers can be extracted by the electron transfer to the TiO_2, separating locally the electrons from the holes. That the remained holes in the $MAPbBr_3$ layer transports to the carbon CE through $MAPbBr_3$ itself. Similarly, TiO_2 compact layer on FTO before TiO_2 mesoporous layer prevents the valence band holes reaching front electrode. The layer cross section SEM image of the device is given in Figure 1. The metal oxide scaffold (TiO_2/Al_2O_3) with a total thickness of about 1.2 μm and mesoporous carbon film thickness of about 10 μm can be easily distinguished. In this study, the TiO_2/Al_2O_3/carbon scaffold is infiltrated with the $MAPbBr_3$ by one-step technique [35]. The $MAPbBr_3$ was deposited by dropping a DMF solution containing different concentrations $MAPbBr_3$ through the top mesoporous carbon CE. Considering the carbon CE total thickness of about 10 μm in this device structure, this step is critical for the finally $MAPbBr_3$ filling process. The homogeneous distribution of $MAPbBr_3$ in the triple-layer structure is illustrated by the EDS image shown in Figure S4. The photocurrent-voltage(*I-V*) curves of the perovskite solar cell tested under 100 mW cm^{-2} AM1.5G simulated solar irradiation are shown in Figure 2a, and the photovoltaic parameters are listed in Table 1. It was found that the TiO_2/Al_2O_3/carbon ($MAPbBr_3$) device displayed a short-circuit current density (J_{sc}) of 6.88 mA cm^{-2}, an open-circuit voltage (V_{oc}) of 1334 mV, a fill factor (FF) of 0.78, achieving a PCE of 7.11%. For comparison, the device with $MAPbI_3$ as absorb layer was also fabricated, showing a lower V_{oc} performance of 970 mV (J_{sc}=17.35 mA cm^{-2}, FF=0.71 and PCE=12.00%).

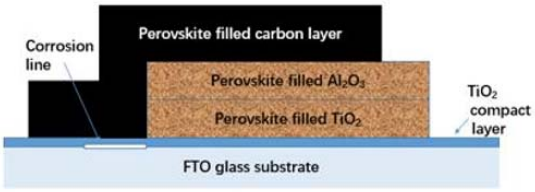

Figure 1 (a): Schematic drawing

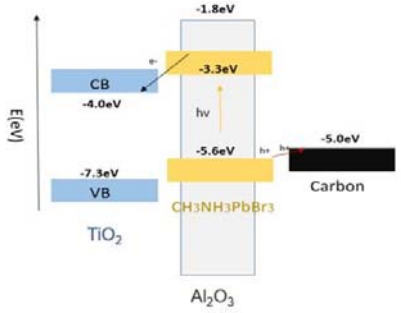

Figure 1 (b): Energy band diagram

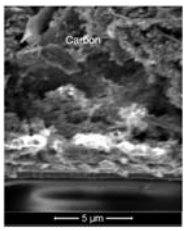

Figure 1 (c): Cross-section SEM

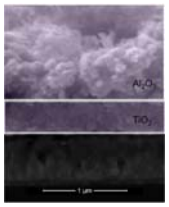

Figure 1 (d): SEM of TiO2/Al2O3 (filled with MAPbBr3) layer

Figure 2b presents the corresponding incident photon to current conversion efficiency (IPCE) curves of the above mentioned two devices. The ~550 nm absorption onset wavelength is consistent with the band gap of $MAPbBr_3$ from figure 1b red line we can acquire. For the device of TiO_2/Al_2O_3/carbon ($MAPbI_3$) spectral response in the wavelength range from 300 to 800 nm. Obviously, the IPCE of TiO_2/Al_2O_3/carbon ($MAPbI_3$) reaches a higher value than the TiO_2/Al_2O_3/carbon ($MAPbBr_3$) device in their spectral response. This agrees with the measured photocurrents values. As shown in Figure 2a, the $CH_3NH_3PbI_3$ perovskite solar cell has a large current density, while $CH_3NH_3PbBr_3$ perovskite solar cell has lower current. From Figure 2b, we can see that the absorption wavelength of the three materials is different for the three materials. Since the band gap of $CH_3NH_3PbI_3$ perovskite is relatively narrow, it can absorb 350~800nm visible light. The $CH_3NH_3PbBr_3$ perovskite band gap is relatively wide, it can absorb 350~550nm visible light. Therefore, there is a huge difference in current density. But band gap of $MAPbBr_3$ material larger than $MAPbI_3$ material, so the full bromine perovskite solar cells will get a relatively high voltage.

After optimizing the $MAPbBr_3$ crystal, we also optimize the thickness of mesoporous TiO_2. This is because the thickness of mesoporous TiO_2 will also affect the performance of the device. So, we studied the influence of different thickness of mesoporous TiO_2 performance to the device. We studied the $MAPbBr_3$ device performance that we made difference thickness of mesoporous TiO_2 with 100 nm, 300 nm, 500 nm, 700 nm.

As shown in figure 3, we can observe the rule that the different TiO_2 thickness affect the performance of device. We can see the influence rule that the different TiO_2 thickness affect the open-circuit voltage from figure 3 (a). The open-circuit voltage will rise with the mesoporous TiO_2 become increasingly thick. This is because when the mesoporous TiO_2 is very thin, the amount of $MAPbBr_3$ in mesoporous too little. Not enough to convert light energy completely. So, the open-circuit voltage will rise with the mesoporous TiO_2 become increasingly thick. While the thickness of the mesoporous TiO_2 increase to 500 nm, the device reached the maximum voltage and most of devices is 1.40 V. But device voltage will fall with the titanium oxide thickness continue to increase. Maybe the device internal defects increase with the TiO_2 thickness increase. Blocking the electron transfer, caused the fall of voltage device. Likewise, the mesoporous TiO_2 thickness will affect the device of short-circuit current and fill factor similarly. As the control of the above conditions, eventually have the same impact on the efficiency of the device. The devices obtain the most superior performance when the mesoporous TiO_2 thickness is 500 nm.

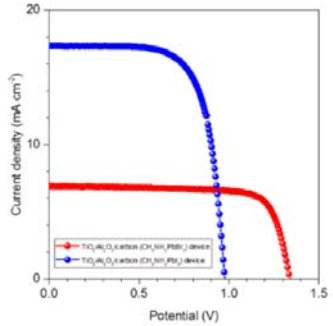

Figure 2 (a): J-V curve

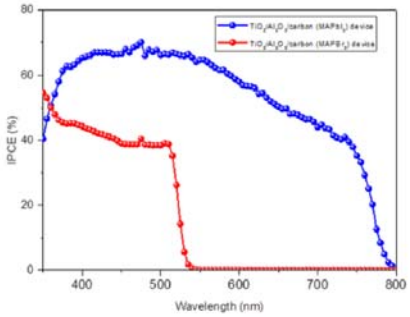

Figure 2 (b): IPCE curve

Table 1: Device performance of TiO_2/Al_2O_3/carbon ($MAPbBr_3$) device and TiO_2/Al_2O_3/carbon ($MAPbI_3$) device

Device	J_{sc} (mA cm^{-2})	V_{oc} (mV)	FF	η(%)
TiO_2/Al_2O_3/C ($MAPbBr_3$)	6.88	1334	0.78	7.11
TiO_2/Al_2O_3/C ($MAPbI_3$)	17.35	970	0.71	12.00

The J-V characteristics at different light intensities can provide charge recombination information inside the battery. There is a linear relationship (as shown in figure 5S) between current density (J_{sc}) and light intensity (I). In other words, as the light intensity increases, the current density increases linearly. This shows that there is no big energy barrier in the TiO_2/Al_2O_3/carbon ($MAPbBr_3$) device structure. The collection of charge has nothing to do with the power of light. Perovskite solar cells of the J-V hysteresis phenomenon that different scanning direction and scanning speed affected the test results often appears during the J-V test. Hysteresis phenomenon is mainly associated with perovskite materials. At the same time, the different of perovskite solar cells' structure can bring about different degree of hysteresis phenomenon. The reasons that cause hysteresis phenomenon are likely to perovskite ferroelectric material itself, capacitive, electronic capture state, ion transport and interface level barriers. For the $MAPbBr_3$ perovskite solar cell, the J-V curve hysteresis phenomenon is not very serious (as shown in figure 4). We think the reason may include: TiO_2/Al_2O_3/carbon ($MAPbBr_3$) perovskite solar cell is a kind of mesoscopic structure. It is advantageous to the collection of the charge that larger interface contact area between $MAPbBr_3/TiO_2$ and $MAPbBr_3$/carbon; The $MAPbBr_3$ material has higher band gap, which is favorable for the charge extraction of the $MAPbBr_3/TiO_2$ interface. At the same time, the $MAPbBr_3$ is a stable cubic structure, with good carrier transport characteristics.

Stability is an important issue for the perovskite solar cells. The organic-inorganic halide perovskite material itself is easily decompose by absorbed moisture, resulting in a rapid decline in performance of the perovskite solar cell. Here, we mainly study the performance attenuation of the $MAPbBr_3$ perovskite solar cell in the non-encapsulated under dark environment (as shown in figure 5a). Test the performance of the $MAPbBr_3$ perovskite solar cell in different placement time. Figure 5a showed the variation of the photovoltaic feature parameters within 1000 hours. After 1000 hours, the perovskite solar cell efficiency didn't decline much. The stability of the device is demonstrated. To further verify the efficiency of the photoelectric conversion of the perovskite solar cell. The steady state power output of the battery is considered a feasible way to evaluate the efficiency of the battery directly. As shown in figure 5b for $MAPbBr_3$ perovskite light-absorbing material

preparation of TiO_2/Al_2O_3/carbon structure device respectively in the mesoscopic PSC J-V curve near the maximum power point, output under constant bias current density with the change of time. As you can see, the current density of the perovskite solar cell is stable to 5.7 mA cm^{-2} after the light starts last 1200s. The results are further illustrated the stability of TiO_2/Al_2O_3/ carbon ($MAPbBr_3$) device.

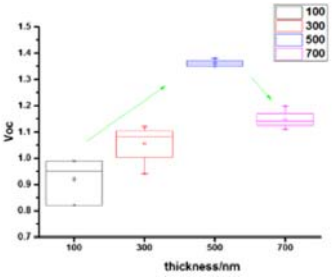

Figure 3 (a): Effect of TiO2 film thickness on Voc

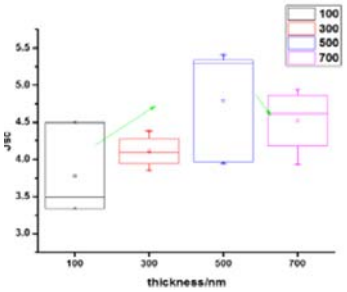

Figure 3(b): Effect of TiO2 film thickness on Jsc.

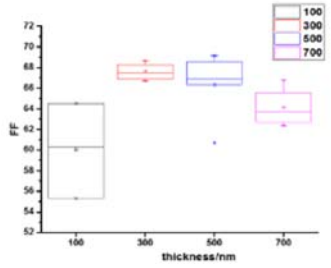

Figure 3(c): Effect of TiO2 film thickness on FF

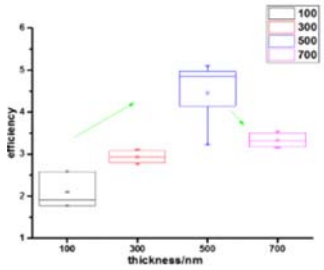

Figure 3 (d): Effect of TiO2 film thickness on PCE

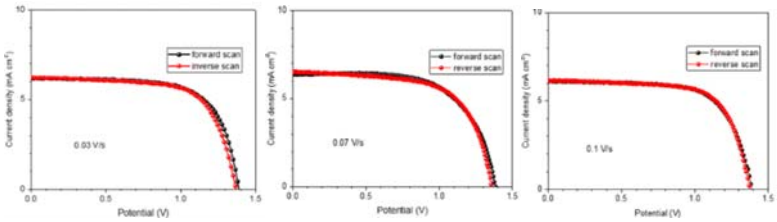

(a) 0.03 V/s, *(b) 0.07 V/s,* *(c) 0.1 V/s,*

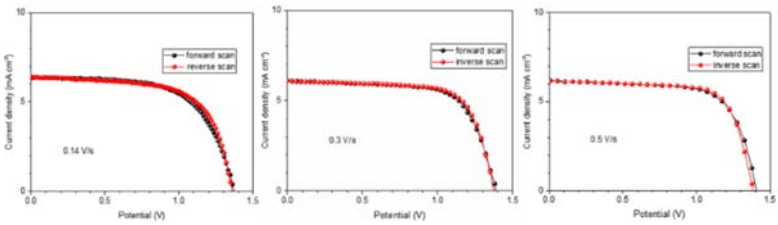

(d) 0.14 V/s, *(e) 0.3 V/s,* *(f) 0.5 V/s,*

Figure 4: Current density-voltage (J-V) curves of TiO_2/Al_2O_3/carbon ($MAPbBr_3$) device at different scanning directions: forward bias scan from 0 V to V_{oc} and reverse bias scan from V_{oc} to 0 V using different scanning rate.

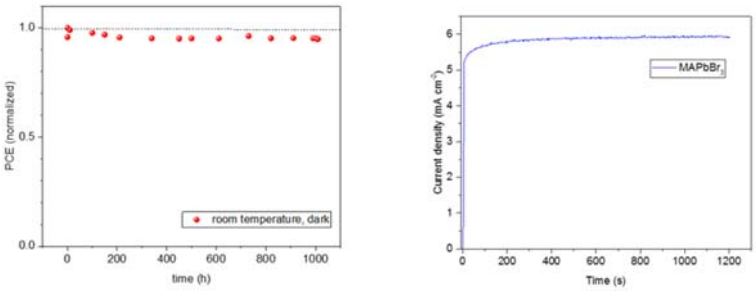

Figure 5: (a) Stability investigation at room temperature in dark. (b) Photocurrent densities as a function of time for PSC devices based on $MAPbBr_3$ perovskite, held at a forward bias of maximum output power point

4. Conclusions

We present $CH_3NH_3PbBr_3$ based solar cell with simplified configuration of FTO/mp-TiO_2/Al_2O_3/carbon via screen printing method. An encouraging V_{oc} of 1.33 V with PCE of 7.11% is obtained giving a promising potential application in water splitting. At the same time, the $MAPbBr_3$ perovskite solar cell showed excellent stability.

Reference

Cao K., Cui J., Zhang H., Li H., Song J., Shen Y., Cheng Y., Wang M., 2015, Efficient mesoscopic perovskite solar cells based on the CH3NH3PbI2Br light absorber, Journal of Materials Chemistry A, 3, 9116-9122, DOI: 10.1039/c5ta01129a.

Li X., Xie F., Zhang S., Hou J., Choy W.C.H., 2015, MoO_x and V_2O_x as Hole and Electron Transport Layers Through Functionalized Intercalation in Normal and Inverted Organic Optoelectronic Devices, Light: Science&Applications,4, e273 DOI:10.1038/lsa.2015.46.

Luo J., Im J., Mayer M.T., Schreier M., Nazeeruddin M.K., Park N.-G., Tilley S. D., Fan H. J., Grätzel M., 2014, Water Photolysis at 12.3% Efficiency via Perovskite Photovoltaics and Earth-Abundant Catalysts, Science 345(6204), 1593−1596, DOI: 10.1126/science.1258307.

Mei A., Li X., Liu L., Ku Z., Liu T., Rong Y., Xu M., Hu M., Chen J., Yang Y., Grätzel M., Han H., 2014, A Hole-Conductor−Free, Fully Printable Mesoscopic Perovskite Solar Cell with High Stability, Science, 345 (6194), 295−298. DOI: 10.1126/science.1254763.

Schreier M., Curvat L., Giordano F., Steier L., Abate A., Zakeeruddin S. M.,Luo J., Maye M.T., Grätzel M., 2015, Efficient Photosynthesis of Carbon Monoxide from CO_2 Using Perovskite Photovoltaics, Nature communications, 6, 7326. DOI: 10.1038/ncomms8326.

Stranks S.D., Eperon G.E., Grancini G., Menelaou C., Alcocer M.J.P., Leijtens T., Herz L.M., Petrozza A., Snaith H.J., 2013, ElectronHole Diffusion Lengths Exceeding 1 Micrometer in an Organometal Trihalide Perovskite Absorber, Science, 342 (6156), 341−344, DOI: 10.1126/science.1243982.